ANTIMICROBIAL ACTIVITY OF GRAPHENE OXIDE-COATED POLYPROPYLENE SURFACES

**LUCIAN CRISTIAN POP[a,c], GABRIEL BARTA[b],
LIVIU COSMIN COTET[a,c], KLARA MAGYARI[c,e], MONICA BAIA[c,d],
LUCIAN BARBU TUDORAN[f,g], RODICA UNGUR[h], DAN VODNAR[b],
LUCIAN BAIA[c,d,e], VIRGINIA DANCIU[a,c*]**

ABSTRACT. Due to its optical, chemical and electronic properties, graphene oxide (GO), among others subtypes of graphene-based materials, has been broadly studied over the past decade. Thanks to its contact-based antimicrobial activity GO represents a good candidate for the construction of materials with antimicrobial properties. Thus, GO's capability to interact with microbes delivers a prospect to improve textiles designed for usage as personal protective equipment. This paper presents the results concerning the obtain of the GO-impregnated SFM-1 polypropylene membrane, its morpho-structure and antimicrobial activity and adherence on two gram-negative bacteria (*E. coli*, *S. thyphimurium*), a gram-positive bacterium (*S. aureus*) and a yeast (*C. albicans*). The investigations on the GO-impregnated polypropylene membrane, through Raman spectroscopy, Scanning and Transmission electron microscopy (SEM, TEM), Energy Dispersive X-Ray Analysis (EDX), X-ray diffraction (XRD), and Fourier-transform infrared spectroscopy (FTIR) suggested the successful polypropylene impregnation with GO. The antibacterial tests have shown that all but one of the microorganisms (*S. typhimurium*) displayed

[a] *Faculty of Chemistry and Chemical Engineering, Department of Chemical Engineering, Babes-Bolyai University, 11 Arany Janos str., RO-400028, Cluj-Napoca, Romania*

[b] *Department of Food Science, University of Agricultural Sciences and Veterinary Medicine, 3-5 Calea Mănăştur str., RO-400372, Cluj-Napoca, Romania*

[c] *Institute of Research-Development-Innovation in Applied Natural Sciences, Babes-Bolyai University, 30 Fântânele str., RO-400294, Cluj-Napoca, Romania*

[d] *Faculty of Physics, Babes-Bolyai University, 1 M. Kogălniceanu str., RO-400084 Cluj-Napoca, Romania*

[e] *Interdisciplinary Research Institute on Bio-Nano-Sciences, Nanostructured Materials and Bio-Nano-Interfaces Center, Babes-Bolyai University, 42 T. Laurian str., RO-400271, Cluj-Napoca, Romania*

[f] *Electron Microcopy Center, Faculty of Biology and Geology, Babes-Bolyai University, 1 M. Kogălniceanu str., RO-400084 Cluj-Napoca, Romania*

[g] *Integrated Electron Microscopy Laboratory, National Research and Development Institute for Isotopic and Molecular Technologies, 67-103 Donat str., RO-400293 Cluj-Napoca, Romania*

[h] *Department of Medical Rehabilitation, Faculty of Medicine, Iuliu Hatieganu University of Medicine and Pharmacy, Louis Pasteur str., RO-400349 Cluj-Napoca, Romania*

* *Corresponding author: virginia.danciu@ubbcluj.ro*

LUCIAN CRISTIAN POP, GABRIEL BARTA, LIVIU COSMIN COTET, KLARA MAGYARI, MONICA BAIA, LUCIAN BARBU TUDORAN, RODICA UNGUR, DAN VODNAR, LUCIAN BAIA, VIRGINIA DANCIU

to be susceptible to the antimicrobial activity of the GO material. Bacterial adhesion was also checked to simulate their affinity for the polypropylene surface immediately after impregnation, in this case the best results were observed on the *S. aureus* strains.

Keywords*: graphene materials; polymer; composite; bacterial adherence, antimicrobial activity.*

1. INTRODUCTION

The increasing resistance of pathogens to antibiotics [1] due to their excessive use has led to the need to find alternative ways to destroy bacteria and fungi based on materials with antibacterial properties such as fullerenes, carbon nanotubes, and graphene [2].

Graphene materials (GM) are crystalline structures formed of carbon nanolayers composed of sp^2 hybridized carbon atoms packed in a honeycomb network [3], creating a 2D crystal [4]. The best-known method of obtaining graphene oxide is the modified Hummers method which is based on the oxidation of graphite with $KMnO_4$ in the presence of H_2SO_4, $NaNO_3$, and H_2O_2 [5]. Recent research has shown that the morpho-structural, optical, and electrical properties of graphene oxide (GO) depend on both the reaction conditions used and the graphite source [6-11].

It has been shown that the antimicrobial activity of GM depends on the presence of various network defects, morphology, number of graphene layers, their lateral size, particle shape, and dispersibility [12], [13]. Thus, Perreault et al. observed that a higher number of defects, respectively smaller GO nanosheets cause an increased antimicrobial activity on *Escherichia coli* [14]. Furthermore, the rise of the number of layers leads to the increase of the GM thickness, which causes a decrease of the nano-knife effect and an increase of the aggregation tendency of the particles. As a result, the contact between graphene and pathogen is reduced [12]. The graphene surfaces angle orientations [15] and the number of free basal planes [16] are also significant parameters influencing the graphene materials' antimicrobial activity. Another important parameter that influences the antifungal activity of graphene material is the shape of the nanoparticles. Sharp-corner protruded particles having a low energy barrier can penetrate more easily through the membrane of the pathogen [17]. According to the literature, there are three main mechanisms by which the antimicrobial activity of GM is manifested, namely:

- the mechanism of nano-knives (cell membrane stress) through which graphene penetrates the cell membrane of the pathogen due to the sharp edges of graphene nanosheets [18]

- the mechanism of oxidative stress that may be dependent or independent on the production of highly reactive species (HRS) [19], [20]

- the mechanism of wrapping/clamping the bacterial cell membrane [21].

The mechanism of oxidative stress independent of the production of highly reactive species is based on the oxidation and destruction of the pathogenic cell by the transfer of charge from the cell membrane to graphene. Initially, oxygen adsorption takes place at the edges of the graphene sheets and in the defective areas, then the reduction occurs through a variety of enzymatic reactions [22-24]. The oxidative stress mechanism, dependent on HRS production, occurs through the intracellular accumulation of OH•, H_2O_2, $^1O_2$, and O_2•- which cause the deterioration of the cell membrane, lipid peroxidation, impairment in the mitochondrial function, and cell necrosis. The mechanism of wrapping / trapping the cell membrane can occur due to graphene's thin and very flexible film structure that surrounds and isolates the pathogen from the nutrient environment, leading, in the end, to the death of the cell [20]. Some researchers have shown that the physicochemical interaction between graphene material and pathogen depends not only on the morpho-structural properties of graphene but also on the structure of the pathogen, the presence or absence of the cell envelope, bacterial cell age, environmental stress conditions, cell metabolism, factors that influence the sensitivity of the bacterium in the presence of GM [25].

In this study, we investigated the antimicrobial activity of the GO obtained by a patented process. We deposited the obtained GO on a polypropylene membrane and then we tested its antimicrobial activity on *Escherichia coli*, a gram-negative bacterium*, Staphylococcus aureus*, a gram-positive bacterium, *Salmonella thyphimurium*, a pathogenic gram-negative bacterium, and *Candida albicans*, an opportunistic pathogenic yeast.

2. RESULTS AND DISCUSSIONS

2.1. Morpho-structural characterization

The structure and properties of graphite oxide depend strongly on method of preparation and degree of oxidation (the quantity of oxygen groups existing on the surface or on the edges). Graphene oxide (Figure1) is the result of liquid phase exfoliation, a procedure in which a single layer or several layers of graphene are exfoliated from graphite in a liquid environment. With attached uncharged but polar oxygen groups such as hydroxyl (-OH) and

epoxide (-O-) and carboxylate groups (-COOH) on the edge and irremediable basal plane defects, the electronic properties of graphene oxide are reduced when related to graphene [18], [25]. The outcome is a huge 2D molecule that has both hydrophilic and lipophilic properties [19] that may behave like a surfactant posseting thus a certain degree of cytotoxicity [20], [21].
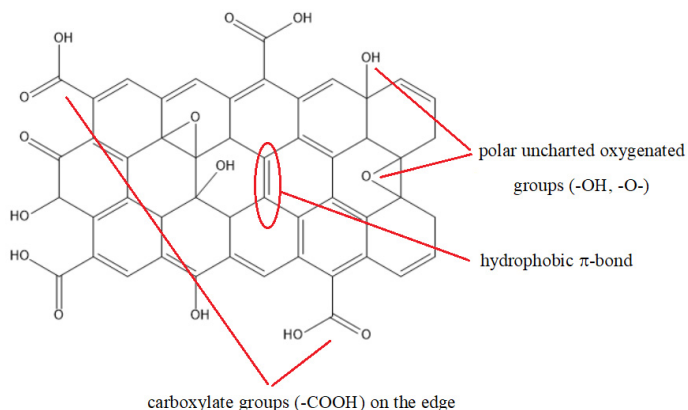

Figure 1. Schematic structure of GO

Raman spectrum of GO-based sample (GO mixed with H_2O: EtOH 1:1) and the spectra of SFM1-PP and SFM1-PP-GO samples were recorded and illustrated in Figure 2. The Raman spectrum of SFM1-PP sample exhibits both the polymer characteristic vibrational bands but also those of the soy flour. Thus, the band at 858 cm^{-1} is due to the stretching vibration of CC and the rocking vibration of CH$_2$ whereas the bands from 1091 and 1100 cm^{-1} are given by the stretching vibration of the CC bonds and the bending vibrations of the CH$_3$. The medium intense band at 1289 cm^{-1} is assigned to the in-plane deformation vibrations of the CH$_2$ groups.

The most intense Raman bands from 1610 and 1722 cm^{-1} are due to the amide I band stretching in the protein secondary structure and carbonyl bond stretching vibrations of the soy flour [26]. The spectrum of GO-based sample exhibits two well-known features: the D band, about 1350 cm^{-1}, due to the structural disorder in graphitic structure, and the G band, at about 1600 cm^{-1}, assigned to the first-order scattering of E2g phonons from sp^2 carbon bonds of the graphite plane [27], [28]. In our spectrum, the D band is located at 1344 cm^{-1}, whereas the maximum of the G band is at 1599 cm^{-1}. The intensity of the D band is correlated with the number of defects in the graphene plan [29]. In the spectrum of SFM1-PP-GO sample one can notice both the presence of bands due to the PP vibrations and the D and G bands specific to GO vibrations, proving the formation of the new composite based on SFM1-PP and GO components.

Considering that the ID/IG intensity ratio can offer information concerning defects in graphene material, we propose evaluating the ratio for the SFM1-PP-GO and GO-based samples. Results previously reported in the literature suggest a link concerning the GO reduction and the rise of the ID/IG intensity ratio [30]. Thus, in order to do this a deconvolution of the spectral range between 1200 and 1700 cm^{-1} of the SFM1-PP-GO spectrum was performed and the obtained bands are illustrated in the inset from Figure 2.
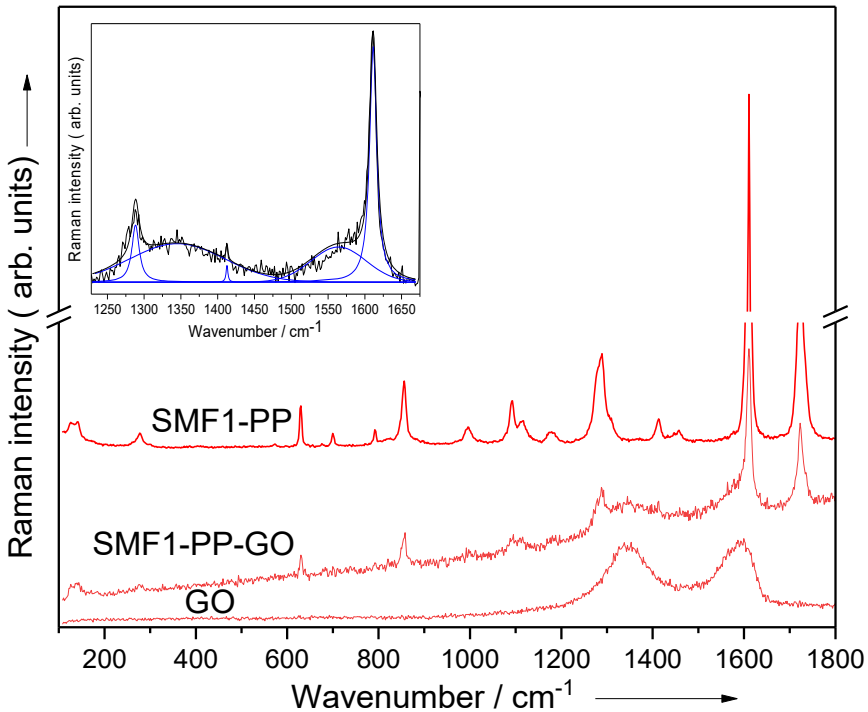

Figure 2. Raman spectra of GO, SFM1-PP and SFM1-PP sample with GO as indicated

Moreover, the ID/IG intensity ratios were calculated, and the same value of 1 was obtained. Thus, in this case, the analysis of the Raman spectra cannot provide detailed information related to the changes of the GO structure that may occur in the SFM1-PP-GO sample as compared to the GO-based one.
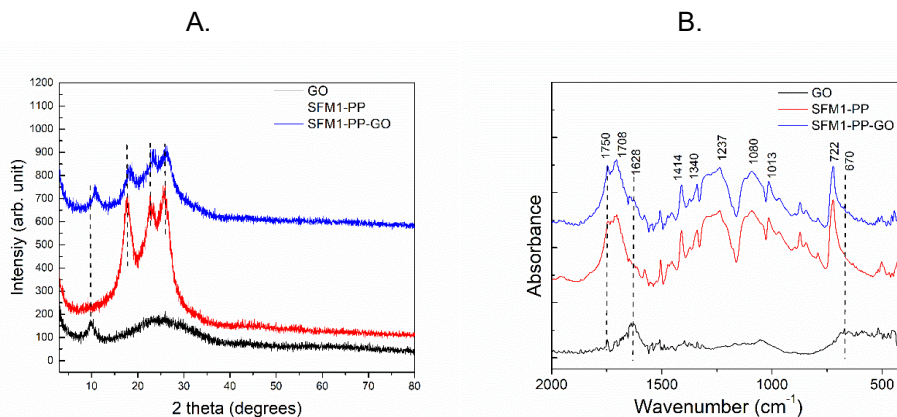
A.   B.

Figure 3. A. XRD analysis of GO, SFM1-PP, and SFM1-PP GO samples,
B. FTIR spectra of GO, SFM1-PP, and SFM1-PP GO samples

The SFM1-polypropylene presents a semicrystalline structure with diffraction peaks coming from (110), (045) and (130) planes (Fig. 3A) [31]. It can be observed that after polypropylene impregnation with GO, the specific GO diffraction peak shift from 9.8° to 10.7° indicating the modification of interlayer spacing which is proportional to the degree of oxidation [32]. This change confirms the binding between the polypropylene material and the GO.

The FTIR spectra of GO and SFM1-PP material, before and after impregnation with GO, were presented in Fig. 3B. The SFM1-PP has characteristic FT-IR spectrum of polyethylene [33] and shows peaks positioned around the following value: 1650 cm^{-1} (carbonyl stretching vibration of the primary amide), 1414 cm^{-1} (bending deformation), 1340 and 1414 cm^{-1} (CH$_3$ symmetric deformation), 1080 cm^{-1} (C-O stretching), 722 cm^{-1} (rocking deformation) [34], [35]. The spectrum of GO presents the following spectral features: C=O stretching (around 1750 cm^{-1}), C=O stretching vibrations from carbonyl group (around 1628 cm^{-1}) and C-O functional group (at 1070 cm^{-1}). After the impregnation of the PP with GO, the FT-IR spectra show all the representative bands of GO, which suggest the successful polypropylene impregnation.

SEM investigations proved a similar diameter of SFM1-PP fibbers ~10 μm (Fig. 4.A) with smooth surfaces and variable sizes of GO sheets spread between polypropylene fibres (Fig. 4.B). The EDX spectra confirmed the presence of GO by differences in S percentage, from the synthesis reactions of GO (Fig. 4 C and D). Side views of GO sheets (Fig. 5.A) and transversal sections (Fig. 5.B) demonstrate a 600-700 nm thickness.
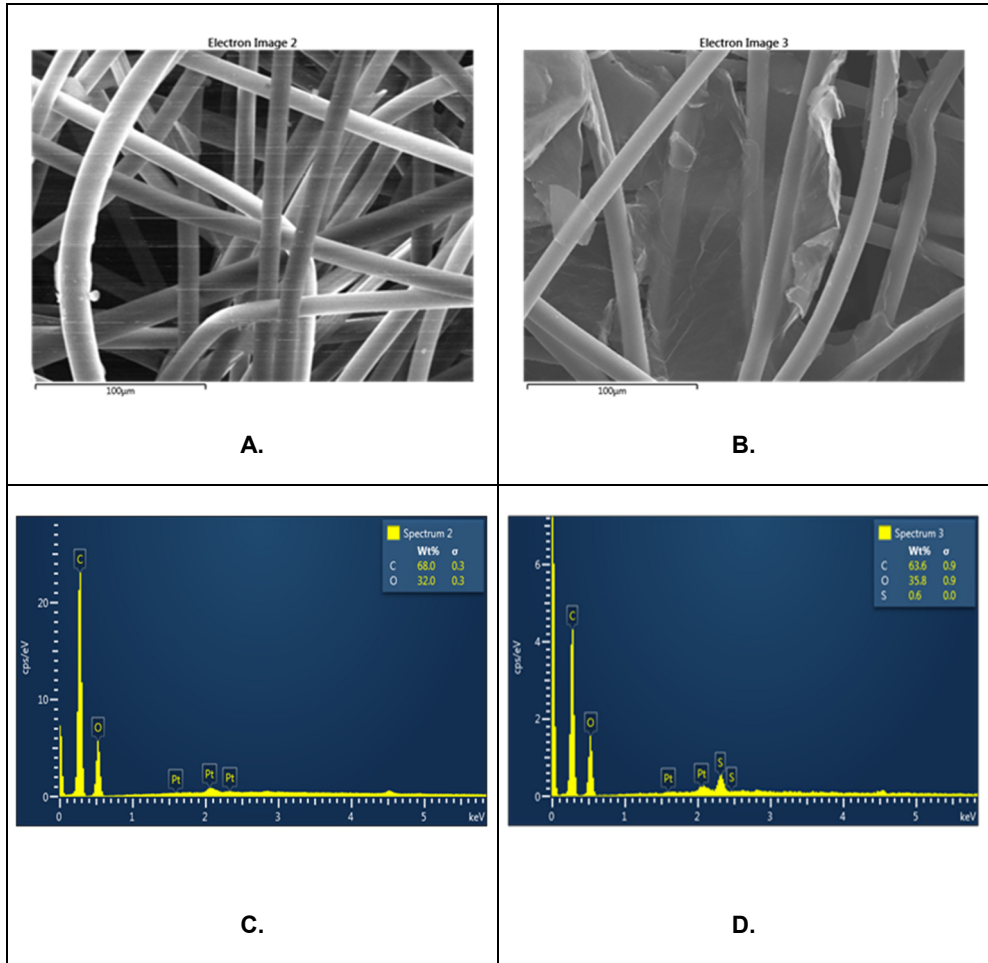
Figure 4. SEM images of the SFM1-PP (A) and SFM1-PP-GO (B), and their EDX spectra (C and D)
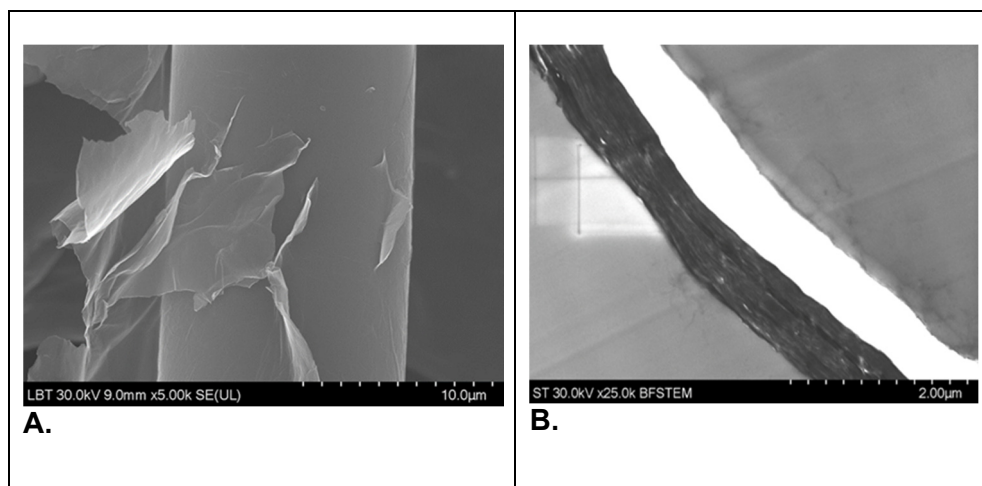
Figure 5. Determination of GO membrane thickness – A. SEM and B. TEM – 600-700 nm

2.2. Antibacterial activity

According to the results determined after counting the number of colonies present on the agar dishes, the activity of the tested samples expressed an antibacterial effect against 3 of the four analysed strains. Initially, the microbial concentrations were at 7 $\log_{10}$ CFU/ml. However, after exposure to the GO-coated polypropylene surface, the final microbial concentrations decreased to 6.11 $\log_{10}$ CFU/ml in case of *E. coli*, 5.84 $\log_{10}$ CFU/ml for *S. aureus*, and 3.54 $\log_{10}$ CFU/ml for *C. albicans*. But in the case of the *S. typhimurium* strain, the samples tested could not inhibit strain development as the number of colonies could not be counted on the agar plates; they did not decrease.

Table 1. Microbial viability after GO exposure

Microorganism	Viability [$\log_{10}$ CFU/ml]
S. aureus ATCC 25923	5.84
E. coli ATCC 25922	6.11
C. albicans ATCC 102310	3.54
S. typhimurium ATCC 14028	-

E. coli and *S. typhimurium* are both gram-negative bacteria having the shape of a rod. The first one has adhesive fimbriae and a cell wall consisting of an exterior membrane having lipopolysaccharides, a periplasmic space with a peptidoglycan sheet, and an internal cytoplasmic membrane [36]. The second one contains characteristics that separate it from other kinds of bacteria. It has 2 membranes (one outside and one inside), periplasm, and a lipopolysaccharide (LPS) [37].

The outer shell of bacteria is negatively charged thanks to the existence of teichoic or lipoic acid in the gram-positive (CW) cell wall or due to LPS and phospholipids in the outer membrane of gram-negative (OM) bacteria [38]. The cytoplasmic membrane (CM) is also negatively charged due to the existence of incorporated phospholipids and proteins. As a result, for adhesion to the surface of the negatively charged cell and subsequent penetration and permeability of the membrane (CM and OM), the graphene material must possess cationic groups and a certain degree of hydrophobicity [39]. The bacterial envelope of the CM and CW membrane functions as an external barrier for the permeability of bacteria. In the case of gram-negative bacteria, the key component of the cell wall is the outer membrane - an asymmetric double lipid layer comprising of proteins, LPS in the outer layer and phospholipids in the inner layer [39].

According to the zeta potential results, the bacterial surface charge of *E. coli* and *S. typhimurium* obtained by T. Arasoglu et al. is -17.9 ± 0.62mV and -13.1 ± 0.57mV [40]. So, it was thought that their interaction with graphene-based material having a positive surface charge is stronger. Furthermore, the pore size of the cell membrane is also important because it is stated in the literature that due to the small pore structure of bacteria, penetration of active substances into the cell is limited [41]. Furthermore, in a recent article, citric acid-coated Fe_3O_4 and Ag nanoparticles had a better antibacterial effect on *E. coli* than on *S. typhimurium* [42], which was also observed in this study, as the GO-coated surface had no significant antibacterial effect on *S. typhimurium.*

S. aureus is a gram-positive cocci-shaped bacterium. One of the primary infection reasons globally is that it can infest diverse host cell types, where it can survive (autophagy and apoptosis) and replicate [43]. At minimal inhibitory concentration (MIC) analysis showed an antibacterial effect similar to *E. coli* strain which was also observable in similar studies but with different antimicrobial polymers/hydrogels. This antibacterial effect was given by the polymers with lower molecular weight (polymethacrylates/polyacrylate, poly-β-lactams, polymalemides, polycarbonates), which can hinder microbial growth even at reduced concentrations [44].

C. albicans is a fungus that is present in various parts of the human organisms and microbiota. Regardless it can also transform in a pathogen, generating life threatening aliment [45]. Because this microorganisms is able to develop in various human tissues it also implies morphological and metabolically alterations related with the manifestation of divergent virulence circumstances (morphogenesis, host recognition biomolecules, secreted phospholipases and proteases) [46]. The highest antibacterial activity in this study was observed with *C. albicans,* which can be bestowed to the membrane integrity disruption and permeabilization given by the GO. The same effect could be observed in a corresponding research with two types of antibacterial peptides on this fungi, which could hinder efficiently the expansion of fungal resistance [47].

2.3. Bacterial adherence

The best bacterial adherence was recorded on the strains *S. aureus*, a gram-positive, round-shaped bacterium, common member of the body microbiota [48], habitually present in the superior respiratory system and on the skin surface. Although *S. aureus* is generally non-pathogenic and living in close association with *Homo sapiens* microbiota, it may occasionally become an opportunistic pathogen, triggering skin and respiratory infections and food poisoning [49]. Pathogenic strains often spread diseases by producing virulence factors.

Table 2. Bacterial adherence to GO-polypropylene sample

Microorganism	Viability [$\log_{10}$ CFU/ml]
E. coli ATCC 25922	uncountable
S. aureus ATCC 25923	4.81
S. thyphymurium ATCC 14028	4.66
C. albicans ATCC 102310	uncountable

The results of this research may have a positive impact against this bacteria's negative effect. Also, positive results were obtained against *S. thyphimurium* on the bacterial adherence tests. Even if the other two bacteria (*E. coli* and *C. albicans*) generated negative effects at adherence, the tested samples showed a slight resistance. Furthermore, the findings of this determination are comparable to those obtained when the sample's minimal inhibitory capacity was examined, as provided with the MIC analysis.

3. CONCLUSIONS

The research presented in this paper supports the further advance of the incorporation of graphene oxide in textiles, taking into account the inhibition effect towards microorganisms. The GO-coated SFM1-PP surfaces developed after an oxidative-exfoliation patented method presented enhanced antimicrobial effect, presumably provided by the small surface size that inhibits the bacterial development and disrupts the bacterial cell membrane. The morpho-structural analyses showed that the graphene oxide sheets having a thickness of 600-700 nm and variable size are spread between the polypropylene fibres. The GO-coated SFM1-PP composite proved effective on 3 of the 4 strains tested, the most affected being the yeast (*C. albicans*).

4. EXPERIMENTAL

4.1. Materials

Reagents were used as received without further purification. Sulfuric acid (H_2SO_4, 98%), phosphoric acid (H_3PO_4, 85%), hydrochloric acid (HCl, 37% aq.), absolute ethanol (C_2H_5OH, 99.5%) were obtained from Nordic Invest, Cluj-Napoca, graphite powder (diameter < 0.15 mm), was purchased from Fluka, potassium permanganate ($KMnO_4$, 99%) was obtained from Merck, hydrogen peroxide (H_2O_2, 3%) was purchased from Hipocrate 2000 based in Bucharest. The microorganisms *E. coli* (ATCC 25922) (gram-negative), *S. aureus* (gram-positive) (ATCC 25923), *S. typhimurium* (ATCC 14028, a pathogenic gram-negative bacterium), and *C. albicans* (ATCC 102310) were procured from Food Biotechnology Laboratory, Life Sciences Institute, University of Agricultural Sciences and Veterinary Medicine, Cluj-Napoca, Romania.

4.2. Methods

4.2.1. Preparation of GO-coated polypropylene sample

The GO suspension was obtained by the patented oxidative-exfoliation method as described previously [50]. In short, a solution of H_2SO_4 and H_3PO_4 (9:1) was added to graphite powder, followed by $KMnO_4$. After the reaction was performed, H_2O_2 was slowly added. Afterward, a few centrifugation-decantation-washing-sonication in H_2O, HCl, and ethanol procedures were carried out. The obtained black-dark product was dispersed in 1:1 volume per volume H_2O/ethanol solution. The installation, shown in Figure 6, was used to obtain the GO-coated polypropylene samples. A 23 mm diameter

disk with an approximate surface of 4.15 cm^2 was made from melt-spun soy flour/polypropylene fibres (SFM1-PP) used to make medical masks. The obtained disk was inserted into a filter funnel, then a few drops of ethanol were poured into moistening the entire surface. Next, 1 ml of a 10 mg/ml GO hydroalcoholic solution (1:1 v/v) was applied uniformly on this surface. After 60 seconds, the water tap vacuum pump was turned on for 60 seconds so that the pores of the material to be filled with GO suspension. The impregnated disk was dried under ambient conditions for 48h yielding a black composite (5.8 mg GO/cm^2). The as-prepared sample was used to test the bacterial adherence and antibacterial activity.
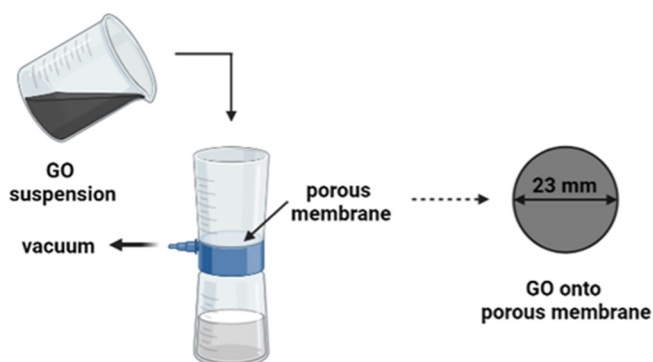

Figure 6. The device used for GO deposition on the SFM1-PP membrane

4.2.2. Morpho-structural characterizations

The FT-IR absorption spectra for all samples were recorded with a Jasco 6200 (Jasco, Tokyo, Japan) spectrometer in reflection configuration, at room temperature, in the range of 400 – 4000 cm^{-1}, with a 4 cm^{-1} spectral resolution; employing the well-established KBr pellet technique.

The X-ray diffraction (XRD) was carried out on a Shimadzu XRD 6000 diffractometer (Kyoto, Japan) using CuKα radiation (λ=1.54 Å), with Ni-filter. The diffractograms were recorded in 2θ range from 3° to 80° with a speed of 2°/min.

Raman spectra were recorded with a Renishaw in Via Reflex Raman Microscope (Wotton-under-Edge, England) equipped with a Ren Cam charge-coupled device (CCD) detector. The 532 nm laser line was used for

excitation, and the spectra were collected with a 0.85 NA objective of 100× magnification. Typical integration times were 10 s, and the laser power was 0.5 mW. The Raman spectra were recorded with a spectral resolution of 4 cm^{-1}.

Morphology and structure of GO and PP fibbers were determined by electron microscopy (EM): for scanning electron microscopy (SEM), samples were deposited onto double sticky carbon tape and sputter-coated with 7 nm of Pt/Pd in an Automatic Sputter Coater (Agar Inc. UK). Images were recorded in a cold field-emission SEM operated at 30 kV (Hitachi SU8320 STEM, Hitachi, Japan), while qualitative and semi-quantitative compositional analysis were obtained using an energy dispersive X-ray spectrometer (EDX) from Oxford Instruments (UK). For transmission electron microscopy (TEM) GO was embedded in Epon 812 (VWR, USA) resin and sectioned at 70-80 nm with a Leica UC7 (Austria) ultramicrotome. Images were recorded in a cold field-emission TEM operated at 200 kV (Hitachi HD2700 STEM, Hitachi, Japan).

4.2.3. Antibacterial activity

To determine the antibacterial activity of the GO-coated polypropylene samples, the guidelines in conformity with the Clinical Laboratory Standards Institute (CLSI) [51] were applied, employing the microdilution method for bacteria that develop aerobically, with minor adaptations [52]. In summary, the microorganisms were cultured in Muller-Hinton Broth (MHB)/Tryptic Soy Broth (TSB), and the cultures were stored at 4 °C and sub-cultured once a month. Preceding antibacterial persistence, C. albicans (ATCC 102310) was cultured in MHB at 30 ℃, and *E. coli* (ATCC 25922), *S. aureus* (ATCC 25923), and *S. typhimurium* were cultivated in TSB at 37 ℃ for 24 h. These cells were washed 3 times with a sterile 0.9% NaCl solution and then diluted to a final density of 7 log10 colony-forming units (CFU) ml-1 in sterile saline solution.

The final density was confirmed by measuring the optical density with the NanoDrop 1000 spectrophotometer (NanoDrop Technologies, Wilmington, DE, USA) at 600 nm (OD600) within the values of 0.009 and 0.011. Then, the cells were brought into contact with the GO-coated SFM1-PP surface for 3 hours. After this incubation period the cell suspension was removed and the GO-coated SFM1-PP filters were washed with sterile 0.9% sodium chloride solution in order to eliminate the unattached cells. After that, the probes were introduced into a 50 ml Falcon vial containing 10 ml of 0.9% NaCl solution followed by a 10-minute sonication period having in mind to remove the cell from the surface. After this operation the cells were immediately placed on agar plates (MHB/TSB) and incubated for the duration of a night at 30/37 °C for the final cell viability determination. Bacteria viability was assessed using plate counting method (viable cell determination within

LUCIAN CRISTIAN POP, GABRIEL BARTA, LIVIU COSMIN COTET, KLARA MAGYARI, MONICA BAIA, LUCIAN BARBU TUDORAN, RODICA UNGUR, DAN VODNAR, LUCIAN BAIA, VIRGINIA DANCIU

30 and 300 colonies/plate) and the values were displayed in logarithmic counts of CFU/ml of sample (log10 CFU/ml). The counting process is described at this reference [53].

4.2.4. Bacterial adherence

The bacterial adherence tests were performed to determine the affinity of microbes to the PP surface straight after impregnation. A procedure modified from Tanner and Nganga [54] has been applied for all the microorganisms tested on coated samples. Each bacterium was precultured from a frozen glycerol preparation and inoculated in a volume of 45 ml MHB over a period of 16 h at 37 °C, respectively, in TSB for 16 h at 30 °C. After this period the bacteria were centrifuged for 10 minutes at 10000 rmp (4 °C), then washed two times with a sodium chloride solution (0.9%). At that point the cells were resuspended in the same solution having a concentration of approximately 0.035 at A550, which corresponded to ~ 1×107 CFU. This suspension was then sonically treated and gently vortexed to homogenize the contents after which was introduced in a 15 ml vial containing 5 ml of the bacterial suspension. Afterward, the samples were washed three times with NaCl solution at ambient temperature followed by a gentle drying procedure so that the surface is not touched. Then, the bacterial samples on the surface of the specimens were collected to perform the viability tests.

Bacterial cells attached to the surface of the samples were collected using micro brushes in tubes with a volume of 2 millilitres containing 0.9 millilitres of MHB/TSB/ with 10% glycerol. Thereafter, the bacterial suspension was homogenized, serially diluted in NaCl 0.9% solution (10 µl of 1:10, 1:100, and 1:1000), and cultured on MHB/TSB agar dishes. CFU measurements were performed after 24 h of culturing at 37/30 ℃.

ACKNOWLEDGMENTS

REFERENCES

1. World Health Organization. Global action plan on antimicrobial resistance. *World Health Organization*, **2017**, 1–28
2. A. Al-Jumaili, S. Alancherry, K. Bazaka, M. V. Jacob, *Materials (Basel),* **2017**, *10*, 1–26

3. B. L. Dasari, J. M. Nouri, D. Brabazon, S. Naher, *Energy*, **2017**, *140*, 766–778

4. K. S. Novoselov, *et al.*, *Nature*, **2012**, *490*, 192–200

5. A. T. Smith, A. M. LaChance, S. Zeng, B. Liu, L.Sun, *Nano Mater. Sci.* **2019**, *1*, 31–47

6. M. S. Junior, M. C. Terence, J. A. G. Carrió, *J. Nano Res.*, **2016**, *38*, 96–100

7. N. I. Zaaba, *et al. Procedia Eng.*, **2017**, *184*, 469–477

8. H. Yu, B. Zhang, C. Bulin, R. Li, R. Xing, *Sci. Rep.,* **2016**, 6, 1–7

9. A. Romero, M. P. Lavin-Lopez, L. Sanchez-Silva, J. L.Valverde, A. Paton-Carrero, *Mater. Chem. Phys.,* **2018**, *203*, 284–292

10. G. Santamaría-Juárez, *et al., Mater. Res. Express,* **2019**, *6*, 125631

11. L. Richtera, *et al.*, *Key Engineering Materials*, **2014**, *592–593*, 374–377

12. X. Zou, L. Zhang, Z. Wang, Y.Luo, *J. Am. Chem. Soc.*, **2016**, *138*, 2064–2077

13. Y. Zhang, *et al., Nanotechnology*, **2014**, *25 (13)*, 135301

14. F. Perreault, A. F. De Faria, S. Nejati, M.Elimelech, *ACS Nano*, **2015**, *9*, 7226–7236

15. V. T. H. Pham, *et al., ACS Nano*, **2015**, *9*, 8458–8467

16. J. D. Mangadlao, *et al., Chem. Commun.*, **2015**, *51*, 2886–2889

17. Y. Li, *et al., Proc. Natl. Acad. Sci. U.S.A.,* **2013**, *110*, 12295–12300

18. S. Liu, *et al., ACS Nano*, **2011**, *5*, 6971–6980

19. J. D. West, L. J. Marnett, *Chem. Res. Toxicol.*, **2006**, *19*, 173–194

20. J. Li, *et al., Sci. Rep.*, **2014**, *4*, 4359

21. I. E. Mejías Carpio, C. M. Santos, X. Wei, D. F. Rodrigues, *Nanoscale*, **2012**, *4*, 4746–4756

22. X. Lu, *et al., Proc. Natl. Acad. Sci. U. S. A.*, **2017**, *114*, E9793–E9801

23. C. Lu, Z. Lu, Z. Li, C. K. Y. Leung, *Constr. Build. Mater.*, 2016, *120*, 457–464

24. S. Gurunathan, J. W. Han, A. Abdal Dayem, V. Eppakayala, J. H. Kim, *Int. J. Nanomedicine,* **2012**, *7*, 5901–5914

25. V. C. Sanchez, A. Jachak, R. H. Hurt, A. B. Kane, *Chem. Res. Toxicol.*, **2012**, *25*, 15–34

26. O. Guzdemir, A. A. Ogale, *Fibers,* **2019**, *7 (10)*, 83

27. M. T. H. Aunkor, I. M. Mahbubul, R. Saidur, H. S. C. Metselaar, *RSC Adv.*, **2016**, *6*, 27807–27825

28. A. C. Ferrari, D. M. Basko, *Nat. Nanotechnol.*, **2013**, *8*, 235–246

29. L. G. Cançado, *et al. Nano Lett.*, **2011**, *11*, 3190–3196

30. S. Pei, H. M. Cheng, *Carbon N. Y.*, **2012**, *50*, 3210–3228

31. C. A. Stackhouse, S. Yan, L. Wang, K. Kisslinger, R. Tappero, A. R. Head, K. R. Tallman, E. S. Takeuchi, D. C. Bock, K. J. Takeuchi, A. C. Marschilok, *Applied Materials & Interfaces* **2021**, *13* (40), 47996–48008

32. L. C. Cotet, K. Magyari, M. Todea, M. C. Dudescu, V. Danciu, L. Baia, *J. Mater. Chem. A,* **2017**, *5*, 2132–2142

33. C. Akarsu, Ö. Madenli, E. Ü. Deveci, *Environmental Science and Pollution Research*, **2021**, *28*, 47517–47527

34. J. V. Gulmine, P. R. Janissek, H. M. Heise, L. Akcelrud, P*olymer Testing*, **2002**, *21*, 557–563

35. T. A. Aragaw, B. A. Mekonnen, *Environ. Syst. Res.*, **2021**, 10:8

36. N. Dasgupta, C. Ramalingam, *Environ. Chem. Lett.* **2016**, *14*, 477–485

37. H. Kita, H. Nikaido, *J. Bacteriol.*, **1973**, *113*, 672–679
38. M. Caroff, A. Novikov, LPS Structure, Function, and Heterogeneity, in Endotoxin Detection and Control in Pharma, Limulus, and Mammalian Systems, K. L. Williams, Springer, Cham., **2019**, Chapter 3, 53-93
39. L. Izzo, S. Matrella, M. Mella, G. Benvenuto, G. Vigliotta, *ACS Appl. Mater. Interfaces*, **2019**, *11*, 15332–15343
40. T. Arasoğlu, *et al., Turkish J. Biol.*, **2017**, *41*, 127–140
41. D. Sun, *et al., J. Nanoparticle Res.*, **2016**, *18*, 1–21
42. L. Gabrielyan, H. Badalyan, V. Gevorgyan, A. Trchounian, *Sci. Rep.,* **2020**, *10*, 1–12
43. K. E. Watkins, M. Unnikrishnan, *Adv. Appl. Microbiol.*, **2020**, *112*, 105-141
44. M. M. Konai, B. Bhattacharjee, S. Ghosh, J. Haldar, *Biomacromolecules,* **2018**, *19*, 1888–1917
45. C. Tsui, E. F. Kong, M. A. Jabra-Rizk, *Pathog. Dis.*, **2016**, *74*, ftw018
46. R. A. Calderone, W. A. Fonzi, *Trends Microbiol.*, **2001**, *9*, 327–335
47. D. do Nascimento, *et al., Sci. Rep.*, **2020**, *10*, 1–14
48. C. Kumpitsch, K. Koskinen, V. Schöpf, C. Moissl-Eichinger, *BMC Biol.*, **2019**, *17*, 1–20
49. K. Szabo, Z. Diaconeasa, A. Catoi, D. C.Vodnar, *Antioxidants*, **2019**, *8*, 1–11
50. M. Stroe, *et al., Molecules,* **2020**, *25*, 1–11
51. M. P. Weinstein, J. B. Patel, C.-A. Burnhman, B. L. Zimmer, Approval CDM-A.; *M07 Methods dilution Antimicrob. Susceptibility Tests Bact. That Grow Aerob.*, **2018**, *91*
52. B. E. Ştefănescu, *et al., Antioxidants,* **2020**, *9(6)*, 495
53. https://users.aber.ac.uk/hlr/mpbb/index_files/Page299.html
54. J. Tanner, P. K. Vallittu, E. A. Söderling, *J. Biomed. Mater. Res.,* **2000**, *49*, 250–256.